

CHAPTER 35

DIFFRACTION DIAGRAMS FOR DIRECTIONAL RANDOM WAVES

Yoshimi Goda, Tomotsuka Takayama, and Yasumasa Suzuki

Marine Hydrodynamics Division, Port and Harbour Research Institute
Ministry of Transport, Nagase, Yokosuka, Japan

ABSTRACT

Conventional wave diffraction diagrams often yield erroneous estimation of wave heights behind breakwaters in the sea, because they are prepared for monochromatic waves while actual waves in the sea are random with directional spectral characteristics. A proposal is made for the standard form of directional wave spectrum on the basis of Mitsuyasu's formula for directional spreading function. A new set of diffraction diagrams have been constructed for random waves with the proposed directional spectrum. Problems of multi-diffraction and multi-reflection within a harbour can also be solved with serial applications of random wave diffraction.

INTRODUCTION

Since the proof by Penny and Price [1] that the diffraction of water waves by breakwaters can be analyzed with Sommerfeld's solution, wave heights behind breakwaters have been estimated with the aid of several diffraction diagrams [2~6]. The phenomenon of wave diffraction is a typical problem for which the solution of velocity potential can be applied with accuracy. Published as well as unpublished laboratory investigations have provided the proof of the validity of wave diffraction theory. Disagreement between the theory and experiment if any is usually attributed to inaccuracy in laboratory measurements. The only exception is the appearance of secondary waves around the tip of a breakwater owing to an excessive gradient of wave energy density there [7].

Such a success of theory, however, should be accepted with a caution when the theory is applied for sea waves characterized with irregularity. Most of diffraction diagrams currently available are those prepared for monochromatic waves with a single period from a single direction. The irregularity of sea waves especially of directional spreading produces the pattern of wave diffraction quite different from conventional diffraction diagrams. An experimental study by Mobarek and Wiegel [8] seems to be the first in demonstrating the application of directional wave spectrum to diffraction problems, though they did not present general diffraction diagrams for engineers' usage.

Being aware of these facts, Nagai [9,10] constructed diffraction diagrams for sea waves in 1972, which have been utilized by harbour engineers in Japan. Figure 1 is one of his diagrams, which shows the diffraction diagram for sinusoidal (monochromatic) waves in the left half and that for spectral waves in the right half for the opening width

of five times the wavelength; the difference between them is very clear. The directional wave spectrum employed for computation was of SWOP type [11], which is primarily for wind waves. In the present paper, recalculation is made of diffraction diagrams of random waves with a new proposal of directional wave spectrum, which is a modification of the spectrum originally formulated by Mitsuyasu et al. [12]. Though these diagrams were previously published in Japanese [13], slight corrections have been found necessary and they are duly corrected hereon. The present paper also discusses the behaviour of waves reflected by breakwaters, which can be deduced from Sommerfeld's solution as proved by one of the authors [14]. With the above knowledge, the problem of multi-diffraction and multi-reflection within a harbour can be solved numerically.

SPECTRAL CALCULATION OF WAVE DIFFRACTION

Random waves in the sea are described with a directional wave spectrum under the presumption that random wave profiles are the result of linear superposition of infinite number of infinitesimal wavelets with various frequencies and directions. According to this presumption, the spectrum of diffracted waves at a point (x,y) is calculated as

$$S_d(f|x,y) = \int_{\theta_{\min}}^{\theta_{\max}} S_i(f,\theta) K_d^2(f,\theta|x,y) d\theta, \quad (1)$$

where $S_i(f,\theta)$ denotes the directional spectrum of incident waves and $K_d(f,\theta|x,y)$ is the diffraction coefficient at a point (x,y) for waves with the frequency f and the direction θ . The spectrum of diffracted waves is given here in the form of frequency spectrum only, because the directional spreading of diffracted waves is limited by the aperture of the breakwater gap looked from the point (x,y) .

The representative heights of incident and diffracted waves are derived from the zeroth moment of spectrum by the theory of Longuet-Higgins [15]. For example, the significant heights are given by

$$(H_{1/3})_i = 4.0\sqrt{(m_0)_i}, \quad (2)$$

$$(H_{1/3})_d = 4.0\sqrt{(m_0)_d}, \quad (3)$$

where,

$$(m_0)_i = \int_0^{\infty} \int_{\theta_{\min}}^{\theta_{\max}} S_i(f,\theta) d\theta df, \quad (4)$$

$$(m_0)_d = \int_0^{\infty} S_d(f) df. \quad (5)$$

Though the constant of 4.0 in Eqs. 2 and 3 is better replaced by that of 3.8 for waves observed in the sea on the average, it does not affect the coefficient of diffraction for random waves, which is defined as

$$(K_d)_{\text{eff}} = (H_{1/3})_d / (H_{1/3})_i = \sqrt{(m_0)_d / (m_0)_i}. \quad (6)$$

The representative periods of diffracted waves are not necessarily the same with those of incident waves. The change of wave period by diffraction can be estimated by the theory of Rice [16] as

$$K_{dT} = \sqrt{\frac{(m_0)_d / (m_2)_d}{(m_0)_i / (m_2)_i}} \quad (7)$$

where,

$$(m_2)_d = \int_0^{\infty} f^2 S_d(f) df \quad (8)$$

$$(m_2)_i = \int_0^{\infty} \int_{\theta_{\min}}^{\theta_{\max}} f^2 S_i(f, \theta) d\theta df \quad (9)$$

The effect of the wave spectrum upon diffraction coefficient is demonstrated in Fig. 2, which shows the diffraction diagrams of a breakwater gap with the relative opening of $B = 3L$ for oblique incident waves with the angle of approach of 60° . The diffraction coefficient is calculated with the approximate method by superposition of Sommerfeld's solutions for two semi-infinite breakwaters. The upper diagram is for monochromatic waves and uni-directional irregular waves (with frequency spectrum only). The difference between them is small, thus indicating unimportance of frequency-wise irregularity. The lower diagram is for uni-frequency random waves with directional spreading and very random waves with a directional spectrum, which corresponds to the case of $S_{\max} = 10$ to be discussed in the next chapter. The difference between them is small, but the both are quite different from those in the upper diagram. Thus, Fig. 2 indicates that the directional spreading rather than the frequency-wise irregularity is important in the diffraction of random waves.

PROPOSAL OF DIRECTIONAL WAVE SPECTRUM

Functional Form

The directional wave spectrum is generally expressed as the product of a frequency spectrum $S(f)$ and a directional spreading function $G(f, \theta)$, that is,

$$S(f, \theta) = S(f) G(f, \theta) \quad (10)$$

The frequency spectrum $S(f)$ is given the unit of $m^2 \cdot \text{sec}$ or its equivalent one, while $G(f, \theta)$ is normalized so as to yield the unit value without a dimension when integrated over the full range of wave direction.

The functional form of $S(f)$ can be taken as Bretschneider's spectrum [17] modified by Mitsuyasu [18] to satisfy the condition of Eq. 2. Thus,

$$S(f) = 0.257 H_{1/3}^2 T_{1/3}^{-4} f^{-5} \exp[-1.03 (T_{1/3} f)^{-4}] \quad (11)$$

This is a type of two-parameter spectrum designated by an arbitrary combination of significant wave height and period, $H_{1/3}$ and $T_{1/3}$. The modal frequency or the frequency at spectral peak is set to satisfy the following relation:

$$f_p = \frac{1}{1.05 T_{1/3}} \quad (12)$$

This relation was proposed by Mitsuyasu [18] and has been confirmed to be representative of sea waves [19]. Spectral forms other than Eq. 11 are also eligible as the standard spectrum, but the change of frequency-wise spectral form will affect little the diffraction of random waves as suggested by Fig. 2.

As to the directional spreading function, the formula proposed by Mitsuyasu et al. [12] on the basis of their detailed observations seems most reliable at present. In a slightly modified form, it is written as

$$G(f, \theta) = G_0 \cos^{2S}(\frac{\theta}{2}) , \tag{13}$$

where,

$$G_0 = \left[\int_{\theta_{\min}}^{\theta_{\max}} \cos^{2S}(\frac{\theta}{2}) d\theta \right]^{-1} , \tag{14}$$

$$S = \begin{cases} S_{\max} \cdot (f/f_p)^5 & : f \leq f_p , \\ S_{\max} \cdot (f/f_p)^{-2.5} & : f \geq f_p . \end{cases} \tag{15}$$

The term of G_0 is so introduced to normalize $G(f, \theta)$. The directional concentration parameter S has the maximum value at $f = f_p$ and decreases at the both sides of spectral peak.

Selection of S_{\max}

Figure 3 is a demonstration of wave patterns, which shows the contours of surface elevations above the mean water level; the portion of wave troughs is left as blank. This figure is a result of numerical simulation by the principle of linear superposition with the spectrum of Eqs. 10 to 15. The maximum directional concentration parameter S_{\max} is subjectively chosen as 10 and 75, respectively. It will be seen that $S_{\max} = 10$ yields the wave pattern quite random and somewhat resembling that of wind waves, while $S_{\max} = 75$ may corresponds to the wave pattern of swell.

The original proposal of Mitsuyasu et al.[12] for S_{\max} is to relate it with the nondimensional frequency parameter as

$$S_{\max} = 11.5 (2\pi f_p U/g)^{-2.5} , \tag{16}$$

where U denotes the wind speed and g is the acceleration of gravity. Equation 16 is not readily applicable for engineering problems because the design wave height and period are often designated without reference to the wind speed. The knowledge of wave growth depicted in the SMB method suggests that the increase of the parameter $2\pi f_p U/g (= U/C_p)$ is associated with the decrease in the wave steepness H_0/L_0 . Thus, S_{\max} can be assumed to increase as the wave steepness decreases. The assumption is supported by the example of Fig. 3 discussed in the above.

From the above discussions, the authors propose the following values of S_{\max} for engineering applications:

$$S_{\max} = \begin{cases} 10 & : \text{for wind waves,} \\ 25 & : \text{for swell with short to medium decay distance,} \\ 75 & : \text{for swell with medium to long decay distance.} \end{cases} \tag{17}$$

Though the above proposal is somewhat subjective, $S_{\max} = 10$ for wind waves is not without ground because it yields the overall directional distribution almost the same with the law of $(2/\pi)\cos^2\theta$ and the formula of SWOP. Figure 4 shows the nondimensional cumulative curves of wave energy calculated for the directional wave spectrum of Eqs. 10 to 15. The term of $P_E(\theta)$ is calculated by

$$P_E(\theta) = \frac{1}{m_0} \int_{-\pi/2}^{\theta} \int_0^{\infty} S(f, \theta) df d\theta. \quad (18)$$

The diagram can be utilized to allocate the relative wave energy to several wave directions such as expressed in sixteen points bearings. Calculation of $P_E(\theta)$ also yields the approximate relation of

$$\ell = 0.11 S_{\max} : \ell \geq 2, \quad (19)$$

for the type of $G(f, \theta)$ of the following:

$$G(f, \theta) \equiv G(\theta) = \frac{2\ell!!}{\pi(2\ell-1)!!} \cos^2\ell\theta, \quad (20)$$

where $2n!! = 2n \cdot (2n-2) \cdots 4 \cdot 2$ and $(2n-1)!! = (2n-1) \cdot (2n-3) \cdots 3 \cdot 1$.

When applying the above spectrum in shallow water, some correction to S_{\max} is necessary because the phenomenon of wave refraction makes the directional spreading to lessen. Calculation of wave refraction in the water of parallel straight bathymetry has yielded the diagram for the change of S_{\max} in shallow water as shown in Fig. 5. The angle $(\alpha_p)_0$ denotes the incident wave angle to the boundary of deep to shallow waters. As the effect of $(\alpha_p)_0$ is small, the diagram may be utilized for waters of general bathymetry.

RANDOM WAVE DIFFRACTION BY A SEMI-INFINITE BREAKWATER

With the directional wave spectrum specified in the above, the computation of random wave diffraction is straightforward so long as the value of diffraction coefficient for monochromatic waves corresponding to spectral components are computable. The integrals in Eqs. 1, 4, and others are to be evaluated in the form of finite series. The number of frequency components does not need to be great, but the number of directional components should be carefully selected in consideration of the trade-off between the accuracy and computation time. When the diffraction coefficient in the area far distant from the breakwater is to be calculated, a large number of directional components are required.

Examples of the diffraction diagrams of semi-infinite breakwater are shown in Fig. 6 for the case of normal incidence for waves with $S_{\max} = 10$ and 75. The diffraction coefficient of wave heights, or $(K_d)_{\text{eff}}$, is shown with contours of solid lines, while the ratio of wave period is shown with contours of dashed lines. A characteristic feature of Fig. 6 is that the diffraction coefficient takes the value of about 0.7 along the boundary of geometric shadow. This value is about 1.4 times the coefficient of monochromatic wave diffraction. In the sheltered area, the random wave diffraction yields the coefficient far larger than that of monochromatic waves.

An verification of the superiority of random diffraction analysis has been provided by Irie [20] with the wave data at Akita Port. Two wave recorders of inverted echo sounder type were set outside and inside a long breakwater as shown in Fig. 7, and the simultaneous observation was carried out in November and December, 1973. The principal direction of waves incident to the breakwater were read from the images of a radar with the wavelength of 8.6 mm, which is commonly employed in Japan for detection of wave direction since around 1962. During the period of observation, the principal wave direction varied in a narrow range of N85°W to N110°W and the direction of N106°W was employed in the calculation of diffraction coefficient. The result of analysis is summarized in Fig. 8. The observed data were classified by Irie into three categories of dispersive, median, and concentrated wave patterns as judged on the radar image. In the computation of random wave diffraction, the maximum directional concentration parameter of Eq. 17 was subjectively applied for these wave categories with the correction of shallow water effect by Fig. 5. Though the scatter of data makes difficult the assessment of the accuracy of random diffraction analysis, it yields quite reasonable estimates of wave heights behind the breakwater. The monochromatic wave analysis, on the other hand, yields the diffraction coefficient being one half to one quarter of the observed value, thus revealing its inapplicability to the problem of sea wave diffraction.

RANDOM WAVE DIFFRACTION THROUGH A GAP OF BREAKWATERS

Another example of the effectiveness of random diffraction analysis has been given by one of the authors [21]. Wave observation were carried out at three stations in Nagoya Port from 1967 to 1970, which is located at the recess of Ise Bay, Japan. As indicated on the inset of Fig. 9, the stations A and B were positioned outside and inside of a long mole of caisson type. The diffraction coefficient for monochromatic waves at the station B is plotted in this figure for predominant wave period of $T = 3$ sec. The waves diffracted from the east entrance penetrate to the station only when the incident wave direction is from SSSW to SSE, and the waves from the west entrance is appreciable for the incident direction of NW to WNW only. Thus the diffraction coefficient for monochromatic waves is very sensitive to the incident wave direction.

Observed wave records did not exhibit such a directionality, as shown in the example of Fig. 10, where the wave spectra at the stations A and B are compared. The wave direction is estimated as SW from the wind record. As the diffraction coefficient for monochromatic waves is about 0.07, the spectral density of the station B would have been about 1/200 of the density of the station A if the diffraction were to be calculated for monochromatic waves. The observed spectrum at B had the density of about 1/10 to 1/20 of the spectrum at A, and it was nearly in agreement with the spectrum calculated as the random wave diffraction phenomenon although the directional spreading function of $(2/\pi)\cos^2\theta$ was employed in the calculation for the sake of simplicity. The agreement of observed and calculated spectra is an evidence of the necessity of introducing random wave analysis in diffraction problems.

Figures 11 to 14 are the result of the computation of random wave diffraction with the directional spectrum described by Eqs. 10 to 15.

The left half of each diagram is for the change of wave period, while the right half is for the wave height ratio. The abscissa and ordinate are normalized with the opening width B instead of the wave length L . In applying these diagrams, appropriate selection of S_{\max} is to be made and interpolation of the diffraction coefficient from the diagrams for $S_{\max} = 10$ and 75 will be required.

COMBINATION OF WAVE REFLECTION AND DIFFRACTION

In the analysis of wave tranquility in a harbour, wave reflections from quaywalls and other solid structures often become the source of troubles. Breakwaters with vertical faces may also cause additional agitation in the area outside the breakwaters. The height of waves reflected by a semi-infinite rigid breakwater can be estimated by means of the well known Sommerfeld's solution. To illustrate the applicability of the solution, it is rewritten in the following form:

$$F_d(r, \alpha, f, \theta) = F_{id}(r, \alpha, f, \theta) + F_{rd}(r, \alpha, f, \theta) \quad (21)$$

where $F(r, \alpha, f, \theta)$ denotes the dimensionless complex wave amplitude at the point P with the distance r and the angle α from the tip of a semi-infinite breakwater for the incident wave with the frequency f and the direction θ (see Fig. 15). The complex amplitudes F_{id} and F_{rd} are expressed respectively as

$$\begin{aligned} F_{id} &= \frac{1}{\sqrt{2}} \exp[i\{kr \cos(\alpha - \theta) + \frac{\pi}{4}\}] \times [\{C(\gamma_1) + \frac{1}{2}\} - i\{S(\gamma_1) + \frac{1}{2}\}] \\ &= \exp[i\{kr \cos(\alpha - \theta)\}] \\ &\quad + \frac{1}{\sqrt{2}} \exp[i\{kr \cos(\alpha - \theta) + \frac{\pi}{4}\}] \times [\{C(\gamma_1) - \frac{1}{2}\} - i\{S(\gamma_1) - \frac{1}{2}\}], \end{aligned} \quad (22)$$

$$\begin{aligned} F_{rd} &= \frac{1}{\sqrt{2}} \exp[i\{kr \cos(\alpha + \theta) + \frac{\pi}{4}\}] \times [\{C(\gamma_2) + \frac{1}{2}\} - i\{S(\gamma_2) + \frac{1}{2}\}] \\ &= \exp[i\{kr \cos(\alpha + \theta)\}] \\ &\quad + \frac{1}{\sqrt{2}} \exp[i\{kr \cos(\alpha + \theta) + \frac{\pi}{4}\}] \times [\{C(\gamma_2) - \frac{1}{2}\} - i\{S(\gamma_2) - \frac{1}{2}\}], \end{aligned} \quad (23)$$

where,

$$\left. \begin{aligned} \gamma_1 &= \sqrt{\frac{4kr}{\pi}} \cos \frac{\alpha - \theta}{2}, \\ \gamma_2 &= \sqrt{\frac{4kr}{\pi}} \cos \frac{\alpha + \theta}{2}, \end{aligned} \right\} (24) \quad \left. \begin{aligned} C(\gamma) &= \int_0^\gamma \cos \frac{\pi}{2} x^2 dx, \\ S(\gamma) &= \int_0^\gamma \sin \frac{\pi}{2} x^2 dx. \end{aligned} \right\} (25)$$

In the derivation of the second expressions from the first ones of Eqs. 22 and 23, the following equality is employed:

$$\begin{aligned} \{C + \frac{1}{2}\} - i\{S + \frac{1}{2}\} &= [\{C - \frac{1}{2}\} - i\{S - \frac{1}{2}\}] + [1 - i] \\ &= [\{C - \frac{1}{2}\} - i\{S - \frac{1}{2}\}] + \sqrt{2} \exp[-i \frac{\pi}{4}]. \end{aligned} \quad (26)$$

As the distance r increases infinitely, the Fresnel integrals defined by Eq. 25 converge to the values listed in Table 1 depending on

the regions in question. Referring to Table 1, it will be readily understood that F_{id} represents the sum of the incident waves and the associated scattered waves, while F_{rd} represents the sum of the reflected waves and the associated scattered waves. Moreover, the primary reflected waves exist only in the region I, whereas the region III is primarily occupied by scattered waves.

Table 1. Behaviour of Fresnel Integrals at $r = \infty$

Region	$C(\gamma_1)$	$S(\gamma_1)$	$C(\gamma_2)$	$S(\gamma_2)$	Primary Waves
I	1/2	1/2	1/2	1/2	incident, reflected, and scattered waves
II	1/2	1/2	-1/2	-1/2	incident and scattered waves
III	-1/2	-1/2	-1/2	-1/2	scattered waves

The above decomposition of Sommerfeld's solution leads to the calculation of reflected waves by means of F_{rd} . If the reflective boundary is finite in its extension, the amplitudes of reflected waves can be approximately calculated by superimposing the two solutions of F_{rd} for the both tips of the reflective boundary as in the technique of calculating wave diffraction through a gap of two semi-infinite breakwaters. For a partially reflective boundary, the coefficient of wave reflection is introduced to linearly reduce the amplitudes of reflected waves. For example, wave pattern around a semi-infinite breakwater with partial wave reflectivity can be calculated by

$$F_d(r, \alpha, f, \theta) = F_{id}(r, \alpha, f, \theta) + K_r F_{rd}(r, \alpha, f, \theta), \quad (27)$$

where K_r denotes the reflection coefficient. Equation 27 remains as an approximation because K_r usually does not carry the information of phase relation except for the cases of $K_r = 1$ and 0.

An experimental verification of the above analysis [14] has been done for the layout of model breakwaters shown in Fig. 16. The breakwaters are made of vertical walls. Incident waves are diffracted by the right breakwater, but some of them are reflected by the rear face of the left breakwater. Experiments were carried out with uni-directional irregular waves, which had the significant height and period of $H_{1/3} = 1.8$ cm and $T_{1/3} = 1.08$ sec; their spectrum could be approximately expressed by Eq. 11. The result of measurements are shown in Fig. 17 for comparison with the theoretical calculation. Good agreement between them is observed except along the line of $x = 8$ m. The difference is due to an assumption employed in the calculation that the source area of wave reflection can be specified by the principle of geometric optics in order to simplify the procedure of calculation. The error due to such simplification is expected to decrease when the directional spreading characteristic of sea waves is introduced.

The analysis of the reflection of diffracted waves can be proceeded for much complicated harbour layout, even though the algorithm needs to be carefully established. Wave diffraction by overlapping breakwaters can also be solved with the knowledge of decomposed Sommerfeld's solution of Eqs. 21 to 23. An example of wave tranquility analysis for a complicated harbour layout is shown in Fig. 18, which represents

the Port of Yokohama in a slightly simplified form. Wind waves with the significant period of $T_{1/3} = 6.0$ sec are considered to come from the direction of SSE. The maximum directional concentration parameter of $S_{\max} = 10$ is employed in the computation. The specification of wave reflectivity of the boundaries is made somewhat subjectively in order to simplify the process of analysis of multi-reflection and multi-diffraction. Though the field data to verify the calculation is not available yet, Fig. 18 demonstrates the capacity of analyzing wave tranquility in a real harbour. It should be noted that the present analysis has no upper bound of application with regards to the size of harbour relative to wavelengths because of the nature of the theory of wave diffraction.

SUMMARY

The present paper has discussed the diffraction of sea waves with directional spectral characteristics. Major conclusions are as follows:

1. The inapplicability of diffraction analysis by monochromatic wave approach has been demonstrated by two examples of field observation data, which at the same time have proved the effectiveness of random diffraction analysis.
2. A standard form of directional wave spectrum is derived on the basis of the directional spreading function proposed by Mitsuyasu et al. Though the selection of directional concentration parameter is left to somewhat subjective judgement of engineers, it can deal with various stages of wind waves to swell.
3. Several diffraction diagrams are presented for a semi-infinite breakwaters and a breakwater gap for the case of normal incidence of directional random waves. The technique can be extended to the case of oblique incidence as well.
4. Sommerfeld's solution of diffracted wave amplitudes is decomposed into the terms of incident, reflected, and scattered waves. The decomposed solutions can be employed for analyzing the behaviour of waves reflected by rigid breakwaters and other reflective structures.
5. Wave tranquility in a harbour of large dimension can be analyzed by serial calculations of random wave diffraction and reflection.

It is mentioned here that the above technique of random wave diffraction analysis is daily utilized by harbour engineers in Japan with the aid of computer program operatable at the Computation Center of the Port and Harbour Research Institute, Ministry of Transport.

REFERENCES

- [1] Penny, W. G. and Price, A. T.: Diffraction of sea waves by breakwater, Artificial Harbour, Dire. Misc. Weapon Tech. His. No. 66, 1944.

- [2] Blue, F. L. and Johnson, J. W.: Diffraction of water waves passing through a breakwater gap, Trans. A.G.U., Vol. 30, No. 5, 1948, pp.705-718.
- [3] Johnson, J. W.: Generalized wave diffraction diagrams, Proc. 2nd Conf. Coastal Engg., Houston, 1952.
- [4] Wiegel, R. L.: Diffraction of waves by semi-infinite breakwater, Proc. ASCE, Vol. 88, No. HY1, 1962, pp.27-44.
- [5] Morihira, M. and Okuyama, I.: Computing method of sea waves and diffraction diagrams, Tech. Note of Port and Harbour Res. Inst., No. 21, 1965, 60p. (in Japanese).
- [6] Takai, T.: The diffraction diagrams of sea waves by a breakwater gap, Tech. Note of Port and Harbour Res. Inst., No. 66, 1969, 42p. (in Japanese).
- [7] Biesel, F.: Radiating second-order phenomena in gravity waves, Proc. IAHR 10th Congress, London, 1963, pp.197-203.
- [8] Mobarek, I. E. and Wiegel, R. L.: Diffraction of wind generated water waves, Proc. 10th Conf. Coastal Engg., Tokyo, 1966, pp.185-206.
- [9] Nagai, K.: Computation of refraction and diffraction of irregular sea, Rept. Port and Harbour Res. Inst., Vol. 11, No. 2, 1972, pp.48-119 (in Japanese)
- [10] Nagai, K.: Diffraction of the irregular sea due to breakwaters, Coastal Engineering in Japan, JSCE, Vol. 15, 1972, pp.59-67.
- [11] Cote, L. J. et al.: The directional spectrum of a wind generated sea as determined from data obtained by the Stereo Wave Observation Project, Meteorological Papers, Vol. 2, No. 6, New York Univ., 1960, 88p.
- [12] Mitsuyasu, H. et al.: Observation of the directional spectrum of ocean waves using a cloverleaf buoy, J. Geophys. Res., Vol. 5, No. 4, 1975, pp.750-760.
- [13] Goda, Y. and Suzuki, Y.: Computation of refraction and diffraction of sea waves with Mitsuyasu's directional spectrum, Tech. Note of Port and Harbour Res. Inst., No. 230, 1975, 45p. (in Japanese).
- [14] Takayama, T. and Kamiyama, Y.: Diffraction of sea waves by rigid or cushion type breakwaters, Rept. Port and Harbour Res. Inst., Vol. 16, No. 3, 1977, pp.3-37.
- [15] Longuet-Higgins, M. S.: On the statistical distribution of the heights of sea waves, J. Marine Res., Vol. XI, No. 3, 1952, pp. 245-265.

- [16] Rice, S. O.: Mathematical analysis of random noise, 1944 and 1945, reprinted in Selected Papers on Noise and Stochastic Processes, Dover Pub., Inc., 1954, pp.132-249.
- [17] Bretschneider, C. L.: Significant waves and wave spectrum, Ocean Industry, Feb. 1968, pp.40-46.
- [18] Mitsuyasu, H.: On the growth of the spectrum of wind-generated waves (I), Rept. Res. Inst. for Applied Mech., Kyushu Univ., Vol. XVI, No. 55, 1968, pp.459-482.
- [19] Goda, Y.: Statistical interpretation of wave data, Draft Contribution to the Committee Rept. I.1 to the 7th Int. Ship Structures Congress to be held in Paris, 1979.
- [20] Irie, I.: Examination of wave deformation with field observation data, Coastal Engineering in Japan, JSCE, Vol. 18, 1975, pp.27-34.
- [21] Goda, Y., Nagai, K., and Ito, M.: Wave observation at the Port of Nagoya (3rd Rept.), Tech. Note of Port and Harbour Res. Inst., No. 120, 1971, 24p. (in Japanese).
- [22] Bretschneider, C. L.: Wave variability and wave spectra for wind-generated gravity waves, U.S. Army Corps of Engrs., Beach Erosion Board, Tech. Memo., No. 113, 1959, 192p.

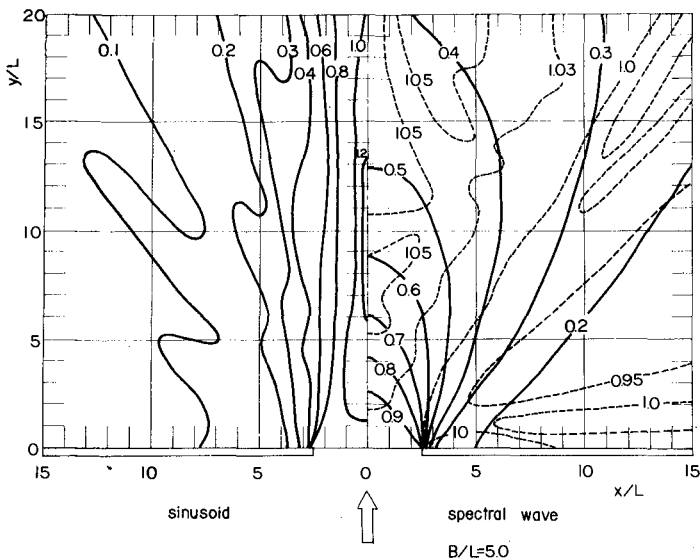
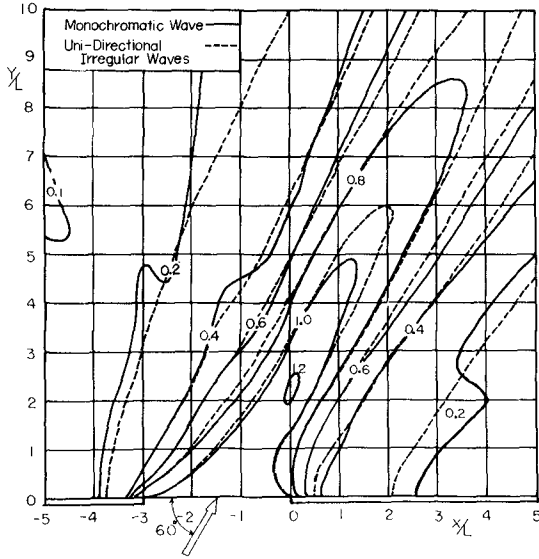
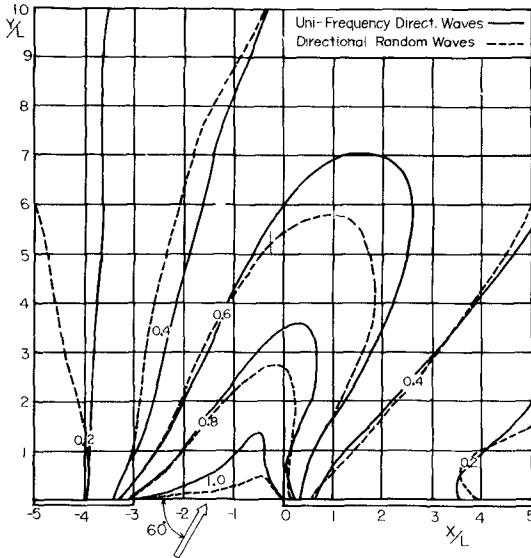


Fig. 1 Comparison of Monochromatic and Random Diffraction Diagrams for the Case of $B/L=5.0$ (after Nagai [9])



(a) monochromatic waves and uni-directional irregular waves



(b) uni-frequency directional waves and directional random waves

Fig. 2 Effect of Directional Spreading Characteristic upon Wave Diffraction through a Breakwater Gap

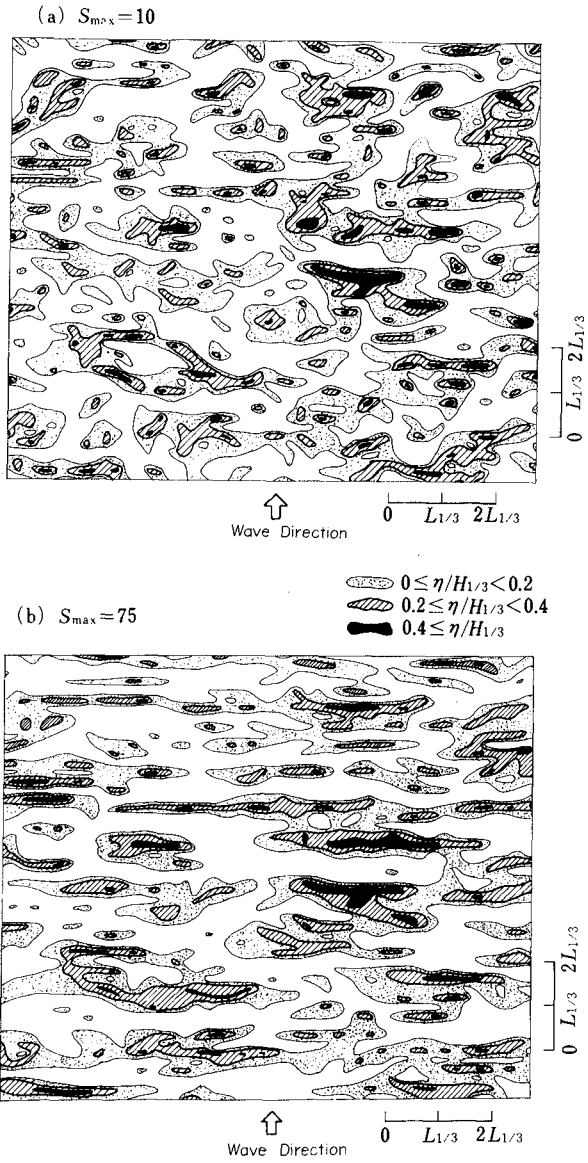


Fig. 3 Surface Elevation Contours of Random Waves by Numerical Simulation

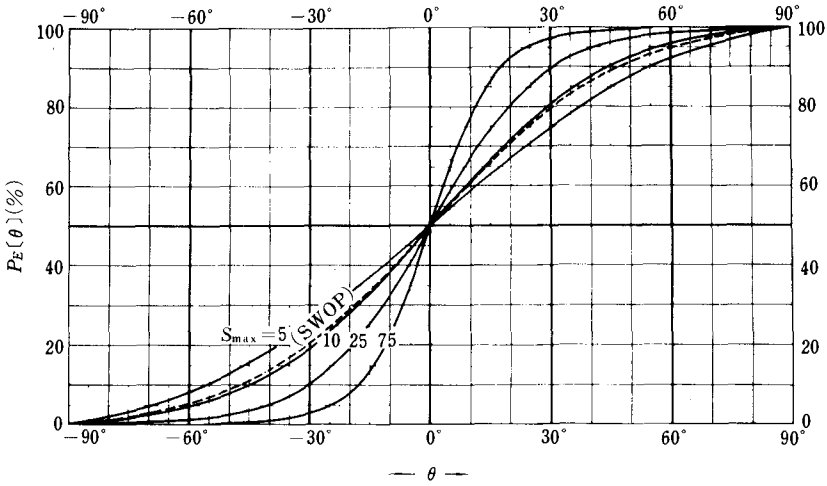


Fig. 4 Cumulative Curves of Relative Wave Energy with Respect to Azimuth from the Principal Wave Direction

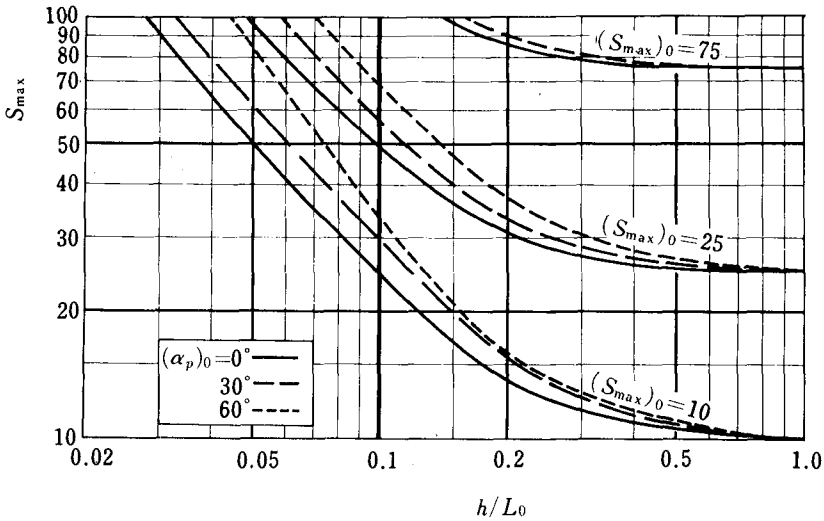


Fig. 5 Change of Maximum Directional Concentration Parameter, S_{max} , Due to Wave Refraction in Shallow Water

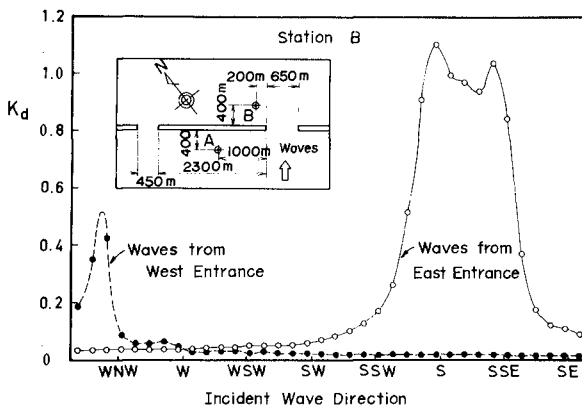


Fig. 9 Diffraction Coefficient by Monochromatic Wave Analysis for the Station B in Nagoya Port

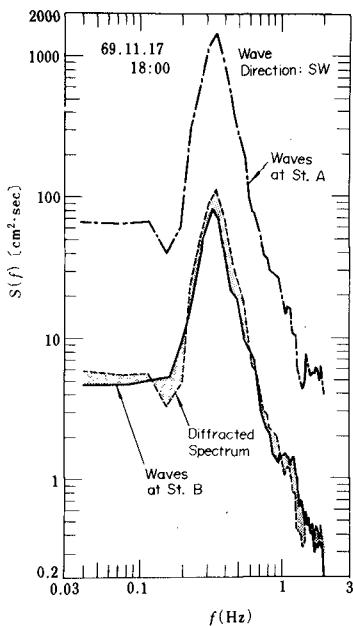
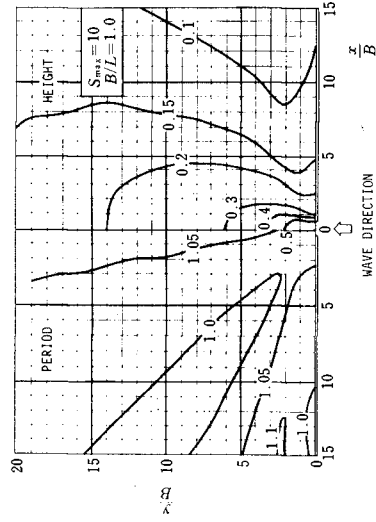
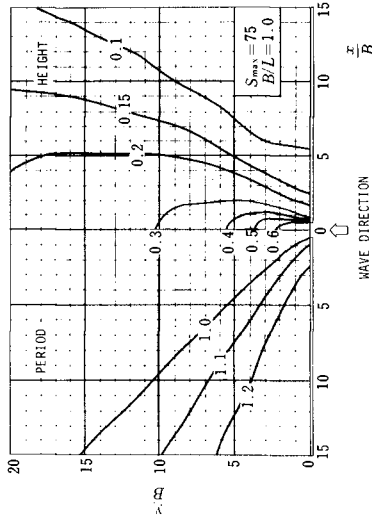


Fig. 10 Wave Spectra Observed at the Stations A and B in Nagoya Port (Wave Direction of SW)



(1) $S_{max} = 10$



(2) $S_{max} = 75$

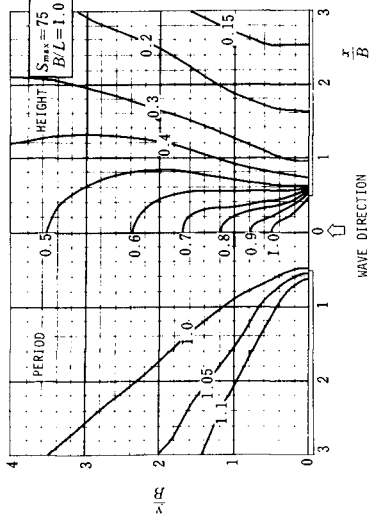
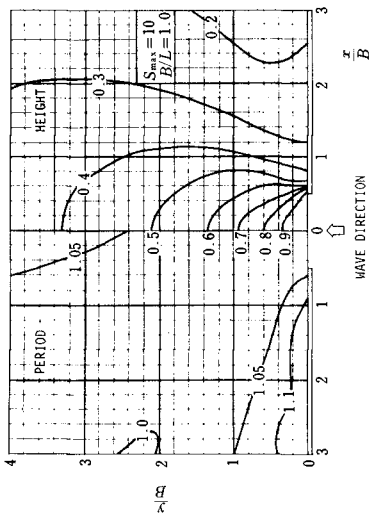
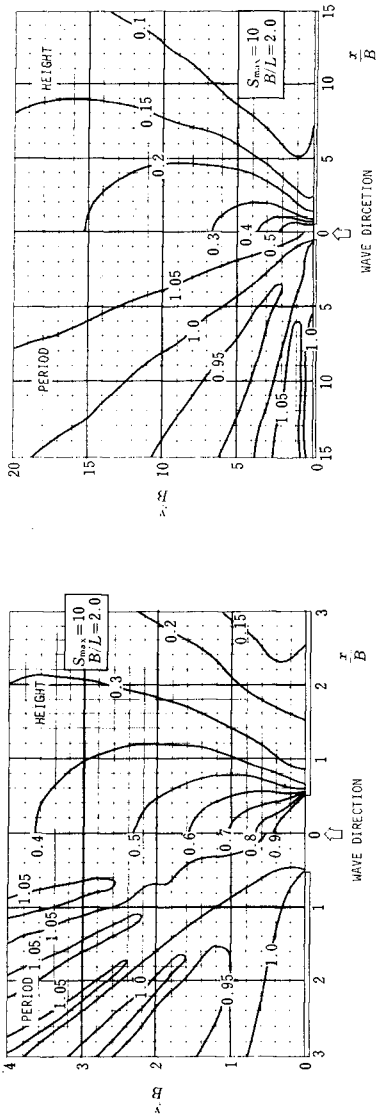
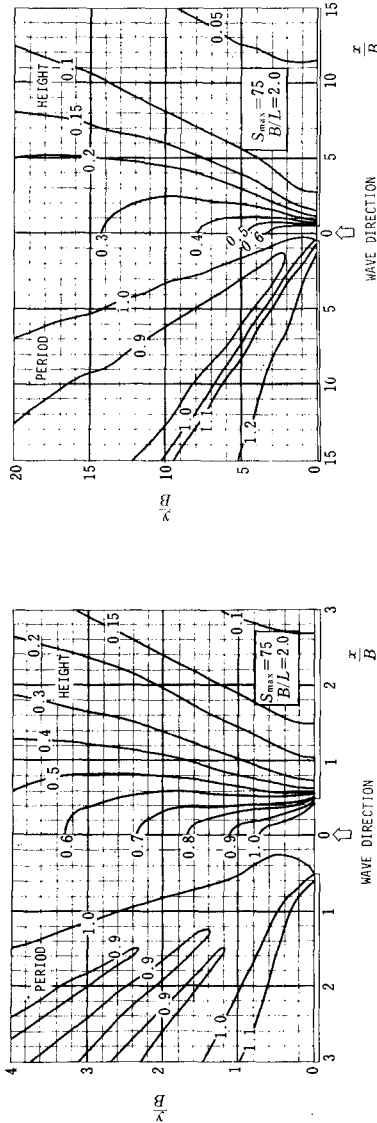


Fig. 11 Diffraction Diagrams of a Breakwater Gap with $B/L = 1.0$ for Directional Random Waves of Normal Incidence

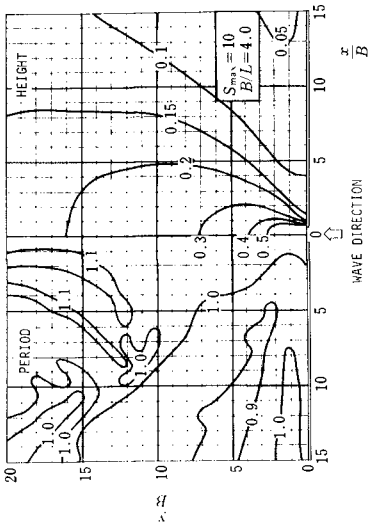


(1) $S_{max} = 10$

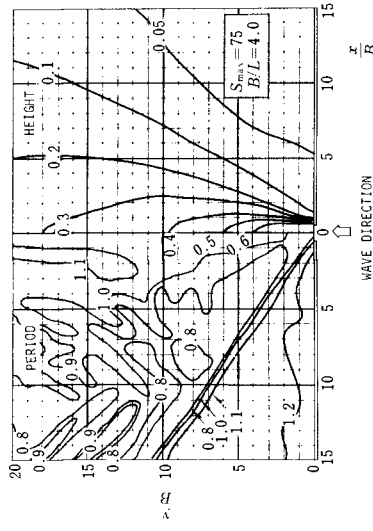


(2) $S_{max} = 75$

Fig. 12 Diffraction Diagrams of a Breakwater Gap with $B/L = 2.0$ for Directional Random Waves of Normal Incidence



(1) $S_{max} = 10$



(2) $S_{max} = 75$

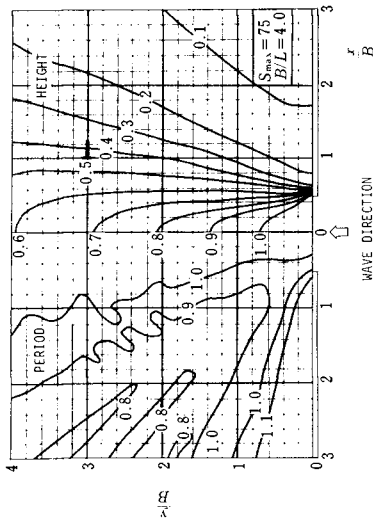
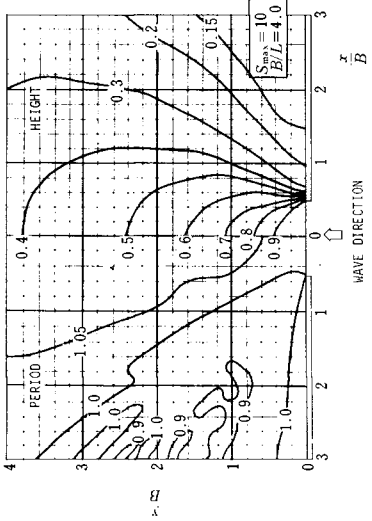
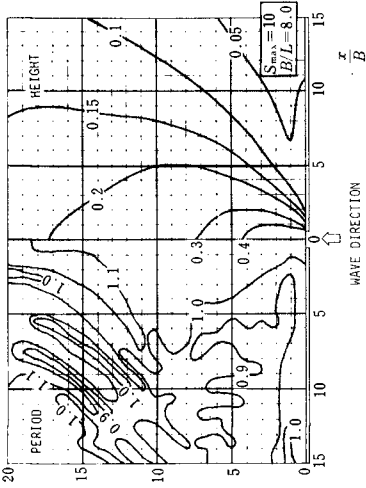
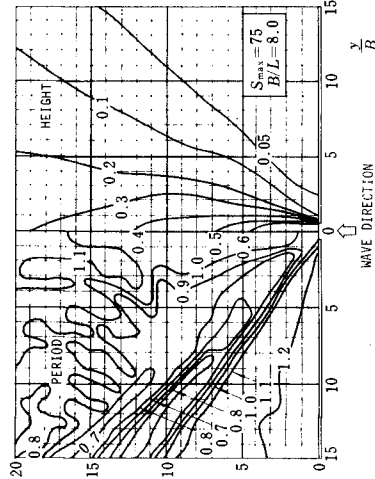


Fig. 13 Diffraction Diagrams of a Breakwater Gap with $B/L = 4.0$ for Directional Random Waves of Normal Incidence



(1) $S_{max} = 10$



(2) $S_{max} = 75$

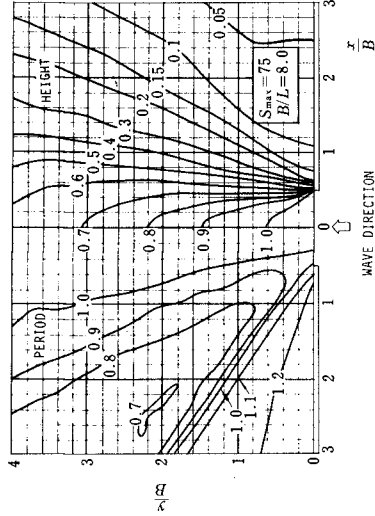
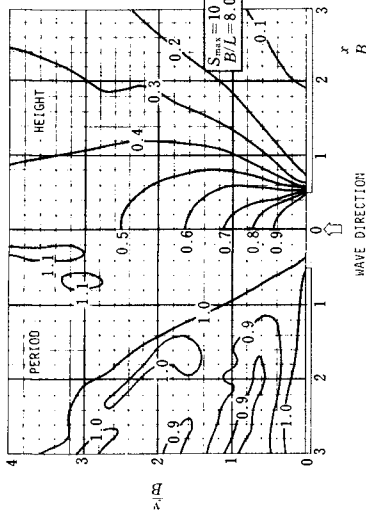


Fig. 14 Diffraction Diagrams of a Breakwater Gap with $B/L = 8.0$ for Directional Random Waves of Normal Incidence

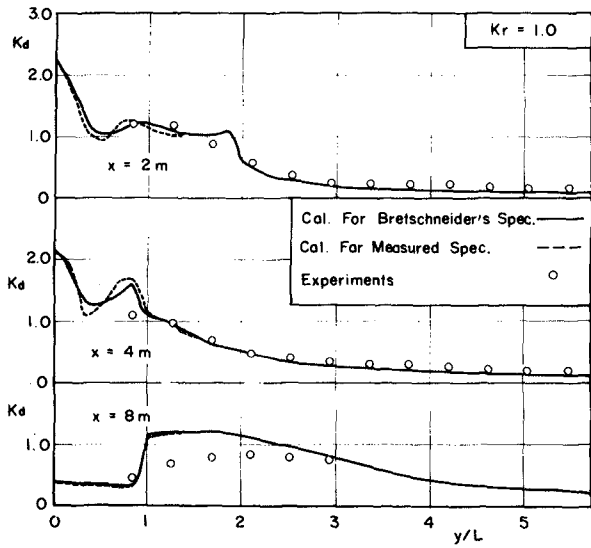


Fig. 17 Measured and Calculated Coefficients of Diffraction by Model Breakwaters

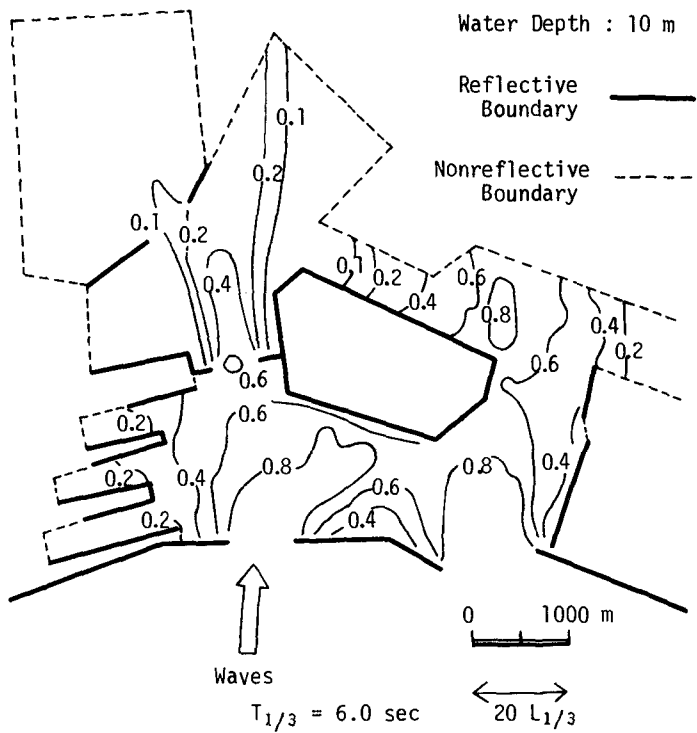


Fig. 18 Estimated Equi-Contours of Wave Height Ratio in Yokohama Port for Wind Waves with $T_{1/3} = 6.0$ sec from SSE